Scanning Microscopy

Volume 10 | Number 3 Article 5

9-7-1996

Application of Monte Carlo Simulations to Critical Dimension Metrology in a Scanning Electron Microscope

Jeremiah R. Lowney
lowney@apollo.eeel.nist.gov

Scanning Microscopy, Vol. 10, No. 3, 1996 (Pages 667-678) 0891-7035/96$5.00+.25
Scanning Microscopy International, Chicago (AMF O'Hare), IL 60666 USA

APPLICATION OF MONTE CARLO SIMULATIONS TO CRITICAL DIMENSION METROLOGY IN A SCANNING ELECTRON MICROSCOPE

Jeremiah R. Lowney

Semiconductor Electronics Division, National Institute of Standards and Technology, Gaithersburg, MD 20899

Telephone number: 301 975 2048 / FAX number: 301 948 4081 / E.mail: lowney@apollo.eeel.nist.gov

(Received for publication March 13, 1996 and in revised form September 7, 1996)

Abstract

The state of the art in Monte Carlo simulations of scanning electron microscope (SEM) signals is reviewed. Two Monte Carlo computer codes were written to simulate the transmitted-, backscattered-, and secondary-electron signals from targets in a scanning electron microscope. The first, MONSEL-II, is applied to semi-infinite lines produced lithographically on multi-layer substrates. The second, MONSEL-III, is an extension to fully three-dimensional targets. Results for a 1 μm step, etched in a silicon substrate are compared with experimental data. The comparisons show that it is possible to obtain edge locations to an uncertainty of less than 10 nm. Simulations were performed for photoresist lines on a silicon substrate coated with a layer of photoresist. Techniques were derived for simulating signals for finite beam diameter from those for zero beam diameter, and for extracting signals approximating zero beam diameter from those with finite beam diameter. Approaches were formulated for efficient use of the Monte Carlo codes.

Keywords: Critical-dimension metrology, linewidth, lithography, Monte Carlo, scanning electron microscope.

Introduction

There is an urgent need to reduce the uncertainty of critical-dimension (CD) measurements in the fabrication of advanced semiconductor devices. This area has been selected as a critical requirement for future devices by the Semiconductors Industry Association [27]. The scanning electron microscope (SEM) is one of the most promising tools to obtain measurements of linewidths to the 10 nm level of uncertainty or better. However, to achieve this level of uncertainty, three conditions must be realized: (1) the measurements must be made very carefully in a properly functioning high-resolution SEM; (2) a computer model is needed to simulate the interactions between the electron beam and the specimen; and (3) a model is also needed to simulate signal detection and instrument signal shaping along with analysis of the performance of the instrument. A review is given of the state of the art in Monte Carlo simulation, after which specific work of the author is presented.

A computer code, MONSEL-II [12], has been written by the author to simulate the interactions between the incident electron beam and specimen and between the collected electrons and the detector. It simulates transmitted-, backscattered-, and secondary-electron images for lines on a multilayer substrate. It includes provision for transmitted- and backscattered-electron detectors, and makes the assumption that all secondary electrons are collected.

A second code, MONSEL-III [14], has just been completed as well. It treats lines of finite length and thus, can show corner as well as edge effects. It also treats via holes and tilted substrates and displays a full two-dimensional signal plot for a two-by-two array of the modeled specimen.

Comparisons have been made between measurements of images produced in the backscattered- and secondary-electron modes and the simulations. Line-edge positions have been obtained at or below the 10 nm level of accuracy by overlaying theoretical and experimental signal traces. Edge slope, roughness, and rounding can cause a smearing of the signal, but the accuracy was not

significantly degraded for the etched step in a silicon substrate used in this work. Simulations were also made for backscattering from photoresist lines on a silicon substrate coated with a layer of photoresist used as an antireflection coating.

A recent study has been performed by the author of the ability to model the SEM signal from a target specimen produced by an incident electron beam with a finite beam diameter by using a superposition of simulations made with an incident beam with zero beam diameter. The zero-beam-diameter simulations are spaced equally across a line edge, and the maximum separation of beam positions is found that retains all the features observed as the beam traverses the edge. This set of solutions, which depends on edge profile and electron-beam energy, can then be used to produce the signal for a finite beam diameter. A method is also derived for extracting data corresponding to zero beam diameter from data obtained with a finite beam diameter. Finally, approaches for efficient use of Monte Carlo codes are formulated.

Review of past work

Modeling the interactions between electron beams and solids has received considerable attention for more than thirty years. There were attempts to develop diffusion models [1], which require randomization of the electron trajectories, as well as single and plural scattering models [26] for thin films. However, these approaches have limitations, and a more accurate approach is to use Monte Carlo methods to simulate the electron trajectories through the solid. Monte Carlo codes are very computer intensive, and the advent of much faster computers has now permitted more extensive use of Monte Carlo methods. The proceedings of a workshop held at National Institute of Standards and Technology (NIST, formerly National Bureau of Standards) in 1975 [21] contains a number of excellent papers describing the early development of Monte Carlo computer codes. The comprehensive book on scanning electron microscopy by Reimer [26] provides many references and furnishes a careful and detailed analysis of the theory behind Monte Carlo methods as well as alternative techniques. The text by Newbury *et al.* [22] reviews Monte Carlo methods although it concentrates mostly on experimental techniques. Joy [7] has made many important contributions to this area and has written a widely used Monte Carlo code [10].

There have been recent advances in Monte Carlo methods with regard to the physics of electron scattering and energy loss, as well as to the geometrical effects associated with the target structure. Two workshops, held under NIST sponsorship, focused on electron-beam/specimen interaction modeling for metrology and microanalysis in the SEM. The workshop papers [2, 4, 6, 8, 13, 18, 19, 20, 23, 25, 28] demonstrated the high level of capability possessed by modern Monte Carlo codes to simulate SEM and associated microanalytical signals.

The second workshop concentrated on comparing Monte Carlo codes from various participants and comparing predictions with measurements. The results of the code comparisons [15] showed major differences among the codes to predict the backscattered- and secondary-electron signals from a test target that consisted of a 1 μm step in a silicon substrate with wall angles of both 1° and 2° from the vertical. The electron-beam energies were between 0.7 and 15 keV. Three of these codes, one of which was MONSEL-II, were in general agreement, and the reasons for the disagreement of the five other codes ranged from limitations in the formalisms for electron scattering and secondary generation, as well as in taking target geometry fully into account. It was recognized that there are trade-offs between codes that have all of the features needed to perform complete simulations and those that are less robust but run faster on work-stations. The comparisons with measurements appears in **Comparisons with Measurements**, below. The success of these workshops has led to a third on electron/instrument interaction modeling in the SEM held at Scanning 96 in Monterey, CA.

Materials and Methods

An electron from the incoming beam in a SEM enters the target and scatters off the atoms before either losing all its energy or emerging from the target. It also can generate other electrons called secondaries. The SEM image is produced from the collected transmitted, backscattered, or secondary electrons as the beam scans the target. Thus, the image is material dependent, and a model is needed to relate the image to the target geometry. Measurements discussed in the following section were made in a high-resolution field-emission SEM, with care taken to obtain images that could be modeled properly by the Monte Carlo codes [17].

The first computer code discussed, MONSEL-II, described in detail elsewhere [12, 14, 17], is for two-dimensional semi-infinite lines on a multilayer substrate. The code simulates linewidth measurements carried out on parallel lithographic lines on top of a substrate with up to three layers placed in a SEM used in the secondary-, backscattered-, or transmitted-electron detection mode. Each line is trapezoidal in cross section, with the possibility of a jog symmetrically located along both edges to study surface roughness. A positive wall angle implies that the line is smaller at the top than at the bottom. The layers and line can have up to nine constituent chemical elements.

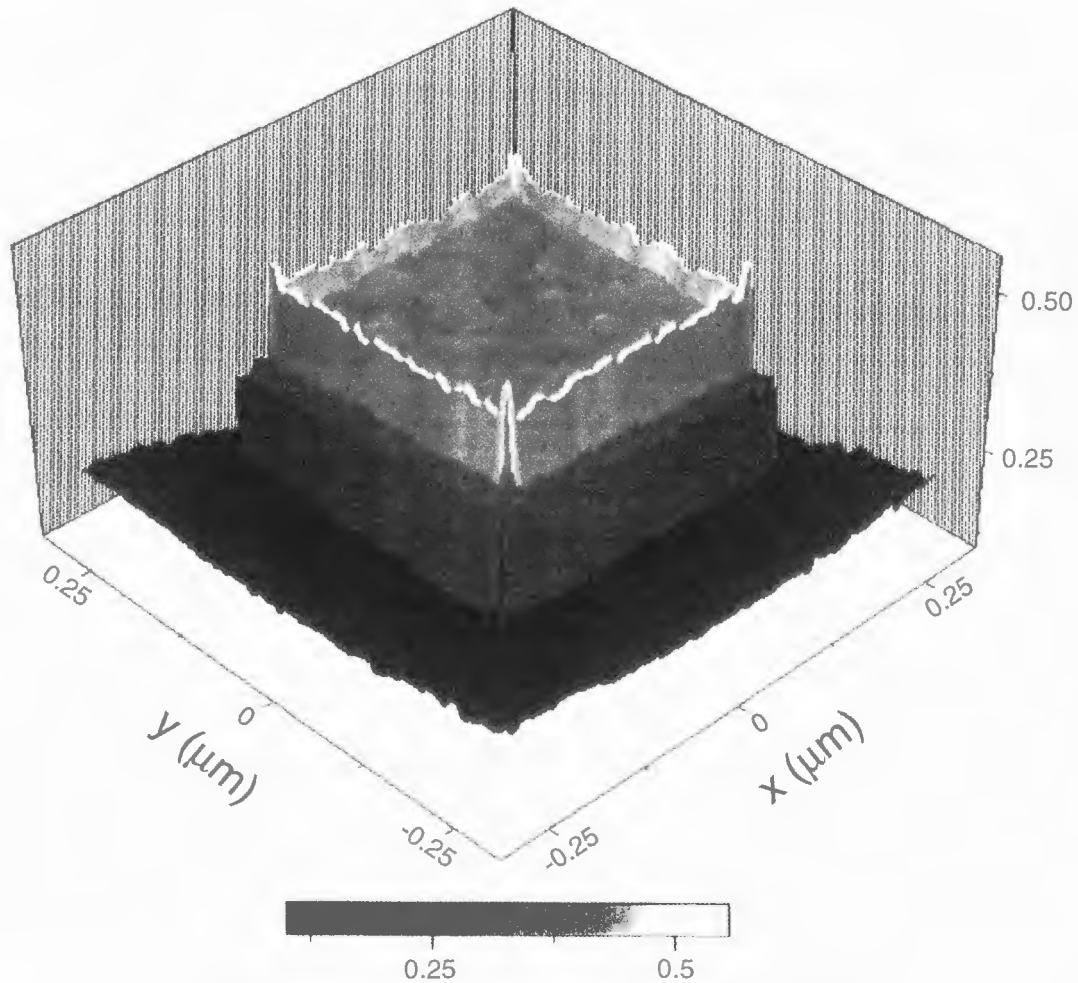

Figure 1. Simulated backscattering coefficient as a function of positions x and y for a gold line, 700 nm high, 250 nm long, and 250 nm wide, on a silicon substrate. The beam energy is 1 keV. The spacing between lines is 250 nm, the beam diameter is 10 nm, and the wall angles are all 88°.

In MONSEL-II, the elastic scattering of electrons is given by Browning's fit to the Mott cross section [3]. Inelastic scattering is treated by using Møller's formula for ionization of valence electrons [17, 26] and Kotera's formalism for plasmon generation [11]. Only undamped plasmons are included so that the plasmon pole approximation may be made [14]. The energy loss rate is from the Joy-Luo [10] modification of Bethe's formula. For electron energies below 50 eV, extrapolation, down to energies below which the formula would predict no energy loss, is used. These energies are close to 1 eV above the work-function energy. This approach is necessary because simple loss-rate formulas are not available for these low energies. A small constant residual energy-loss rate is added to the Joy-Luo [10] formula so that the loss rate is positive at all energies. It is adjusted to obtain measured secondary yields. Individual trajectories are used throughout, and intersections with all the sample boundaries are computed. Provision exists for the limited collection of transmitted and backscattered electrons by detectors, but all secondaries are assumed to be collected.

The second code, MONSEL-III [14], performs the same functions as MONSEL-II but simulates fully three-dimensional (3D) targets. The model target is a two-by-two array of identical lines or via holes with trapezoidal faces. No jogs are currently implemented along the faces, but the target can be tilted relative to the beam. The calculation of boundary crossings is streamlined relative to the method used in MONSEL-II. All the faces are numbered as well as the distinct regions in the substrate from which an electron can emerge. The calculations of the intersections are all done in a separate subroutine, and an input file is used to determine which

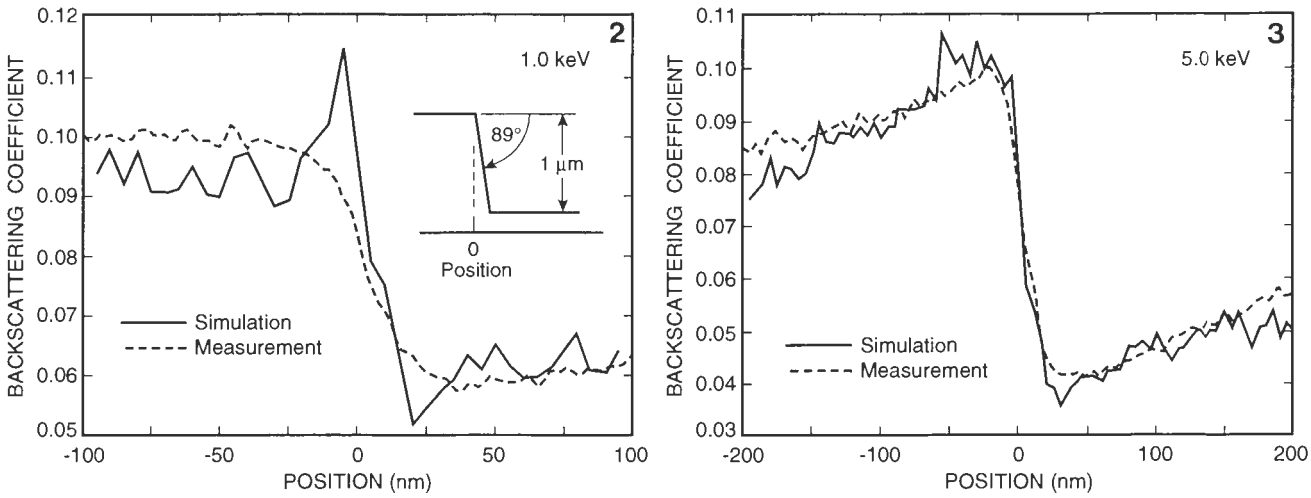

Figures 2 and 3. Backscattering coefficient as a function of position for a 1 μm step in a silicon substrate. The simulation is given by the solid line and the measured data by the dashed line. The beam energy is 1 keV (**Fig. 2; at left**) or 5 keV (**Fig. 3; at right**), and the beam diameter is 10 nm. The zero of position is the top of the ledge, and the wall angle is 89°.

faces an electron can enter or reenter and in which order entry or reentry can occur. The code can be easily modified to model other object shapes and can be used to study effects of corners and other 3D phenomena.

An example of a simulation for gold lines on a silicon substrate, as used for X-ray masks, performed with MONSEL-III is shown in Figure 1. The figure represents one quadrant of a two-by-two array of square lines with the front corner taken to be an outer corner. Note the signal enhancement near the top edges of the lines and especially at the corners due to edge emission, and the signal reduction near neighboring lines behind this line due to shadowing. The signal from the substrate (darkest area) is not flat because of interactions of backscattered electrons with the lines.

Results and Discussion

Comparisons with measurements

The results of the MONSEL-II simulations for the edge region of a 1 μm step in a 1 mm thick silicon substrate have been compared with SEM measurements performed on a corresponding sample with a nearly vertical side wall. The sample was specially fabricated and measured on a high-resolution field-emission SEM [16, 24]. The wall angle in the model was measured to be 89°, which is a nearly vertical wall, and thus the base extends 17.5 nm beyond the top of the ledge. There were 10,000 trajectories per point, and all secondary electrons were assumed to be collected. The detector for backscattered electrons had an acceptance angle of 19° to 44°. The beam diameter was taken to be 10 nm.

Figure 2 shows the overlay of the simulated backscattering coefficient and the data at 1 keV beam energy. The data were scaled and shifted to obtain the best agreement by eye. Mathematical procedures for obtaining the best agreement could be developed, but at this stage, it is not clear how to improve on eyeball fits. The zero of position corresponds to the top of the ledge on the substrate. These data do not exhibit the sharp peak at the top of the ledge seen in the simulation. This may be due to surface roughness, which can lead to reabsorption of electrons emitted out the face of the ledge, or surface contamination, which can prevent low-energy electrons from escaping. Overall, the fit is very good, and shifts of more than 5 nm either way result in noticeable disagreement between simulation and data. Thus, even though the data are somewhat smeared out relative to the simulation, it is possible to determine the location of the edge to within 10 nm.

The same comparison for 5 keV beam energy is shown in Figure 3. The agreement is very good, and the estimated uncertainty in edge location is the same as for 1 keV. The signal is broadened at 5 keV because of greater electron penetration, but shifts in position between simulation and data greater than ± 5 nm lead to noticeable disagreement between them.

Figure 4 shows the secondary yield as a function of position for the simulation and corresponding data for 1 keV. The agreement is excellent, and shifts of ± 3 nm lead to noticeable disagreement between simulation and data. Thus, the edge position can be determined to within about 6 nm, which is the smallest estimated uncertainty obtained in this study. This value is below the

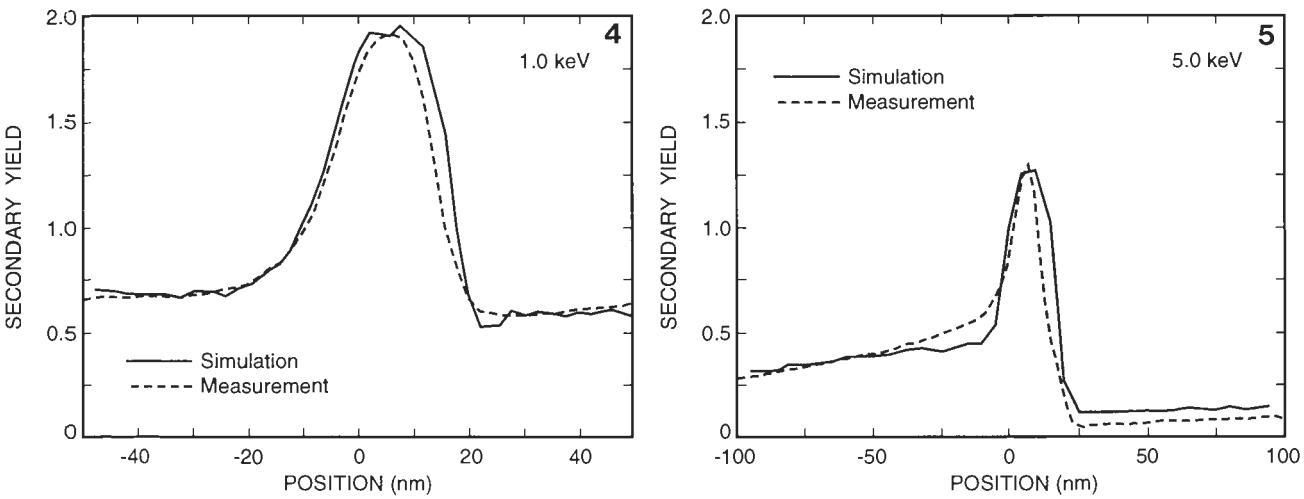

Figures 4 and 5. Secondary yield as a function of position for a 1 μm step in a silicon substrate. The simulation is given by the solid line and the measured data by the dashed line. The beam energy is 1 keV (**Fig. 4; at left**) or 5 keV (**Fig. 5; at right**), and the beam diameter is 10 nm. The zero of position is the top of the ledge, and the wall angle is 89°.

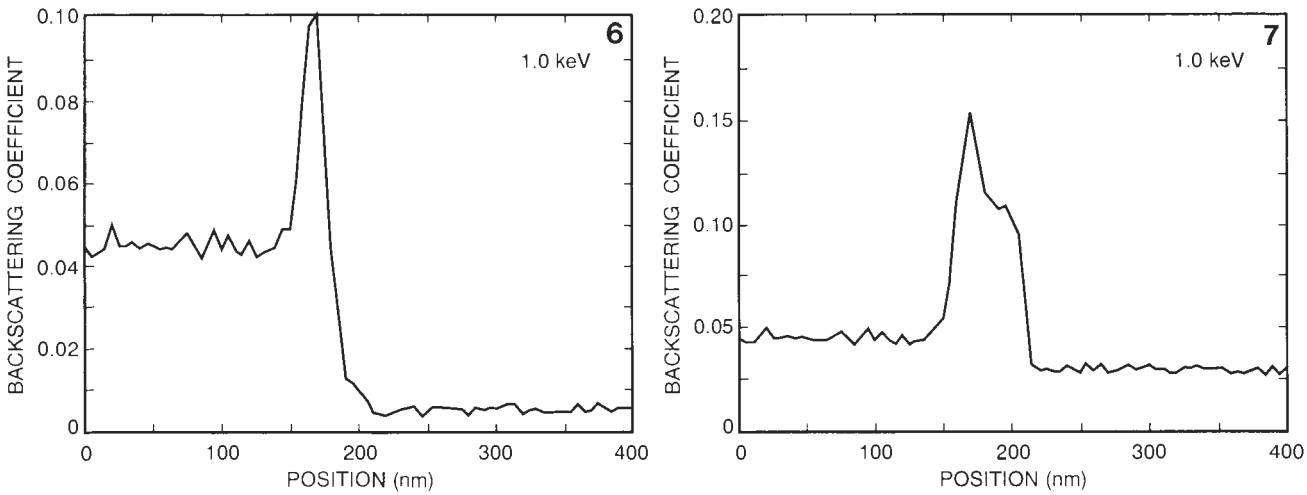

Figures 6 and 7. Simulated backscattering coefficient as a function of position for an inner (**Fig. 6; at left**) and an outer (**Fig. 7; at right**) photoresist line on a silicon substrate with a 60 nm coating of photoresist. The line is 1 μm high and 0.35 μm wide, separated by 0.35 μm from the next line. The beam energy is 1 keV, the zero of position is the line center, and the wall angle is 88°.

---

7 nm uncertainty required for CD metrology by the year 2010 [27]. Figure 5 shows the fit for a 5 keV beam energy, and the agreement is nearly as good, with an estimated uncertainty of about ± 5 nm. However, this analysis represents only one component of the uncertainty associated with the measurement. Therefore, these results show feasibility, but much work still remains to achieve the lowest possible measurement uncertainty in general use.

Simulation of photoresist lines

A common application of SEM metrology is the measurement of photoresist lines on silicon substrates. Figure 6 shows the simulated backscattering coefficient at 1 keV beam energy as a function of position for the central line of three photoresist lines on a silicon substrate. The substrate was coated with 60 nm of photoresist, which acts as an antireflection coating. The lines

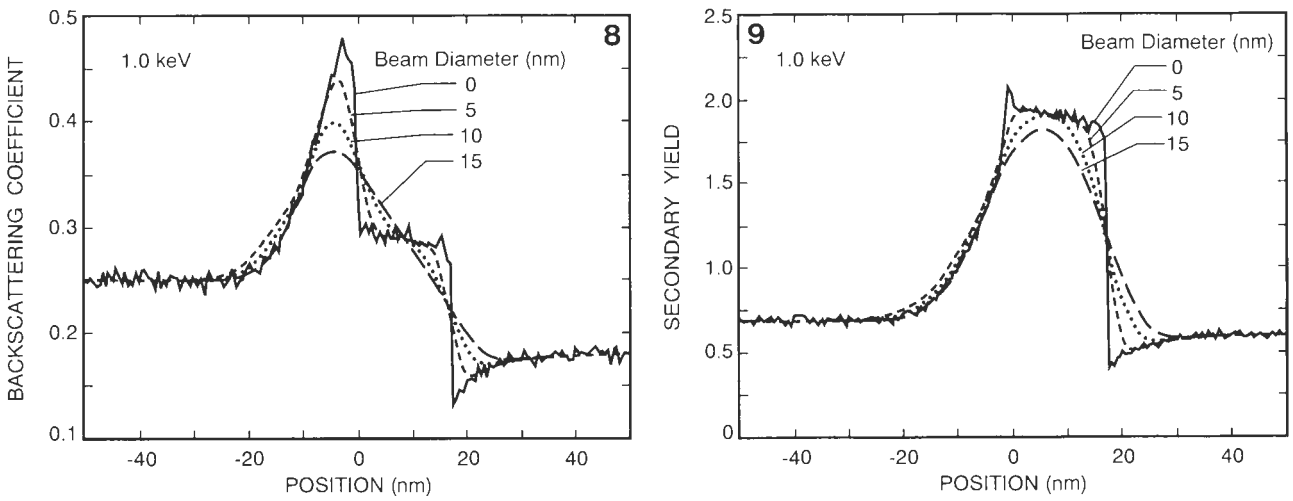

Figures 8 and 9. Simulated backscattering coefficient (**Fig. 8; at left**) and secondary yield (**Fig. 9; at right**) as a function of position for a 1 μm step in a silicon substrate. The beam energy is 1 keV. The solid line is for zero beam diameter, while the succeeding broken lines are for 5, 10, and 15 nm beam diameters, respectively. The zero of position is the top of the ledge, and the wall angle is 89°.

List of Symbols

a	Maximum limit of integral away from electron-beam center
d	Diameter of incident electron beam
m	Number of data points in measured signal
n	Limits maximum number of terms in deconvolution to 2n+1
$s(x_0,d)$	Signal from electron beam with diameter d, centered at x_0
$s(x_i,d)$	Signal from electron beam with diameter d, centered at pixel x_i
$s_0(x)$	Signal from electron beam with zero diameter at position x
$s_0(x_j)$	Signal from electron beam with zero diameter at pixel position x_j
x	Position coordinate of incident electrons in x-direction
x_0	Position of center of electron beam in x-direction
x_i	Position coordinate of pixel located at x_i
y_0	Position of center of electron beam in direction perpendicular to x
C	Normalization constant for discrete representation of signal $s(x_i,d)$

on the substrate are 0.35 μm wide and 1 μm high, with 0.35 μm spacings in between. The zero of position is the center of the middle line, and the wall angles were taken to be 88°. The beam diameter was taken to be 16 nm, and the detector acceptance angle was taken to be 45° to 90°. This wide acceptance angle occurs because of electric and magnetic fields that bend the backscattered electron trajectories on the way to the detector in this special SEM design. The backscattering coefficient is greatly reduced in between the lines because of the shadowing effect of the steep walls on either side.

Figure 7 shows the simulation for the same case as in Figure 6, except that it is for an outermost line. The backscattering coefficient is much higher from the substrate because the shadowing is reduced, and the structure associated with traversal of the line edge by the beam is more detailed because of the reduced shadowing. The SEM signal is very sensitive to wall angle, and modeling allows one to obtain an estimate of the angle.

Effect of beam spreading

The detail that can be obtained from a target is affected by the diameter of the incident electron beam, which is assumed to have a Gaussian distribution of electrons about its center, x_0, y_0 [21]. This analysis is restricted to variations only in x because the target is presumed to be invariant in the y-direction in MONSEL-II. The following equations may be easily generalized for a fully 3D as allowed by MONSEL-III. Thus, the

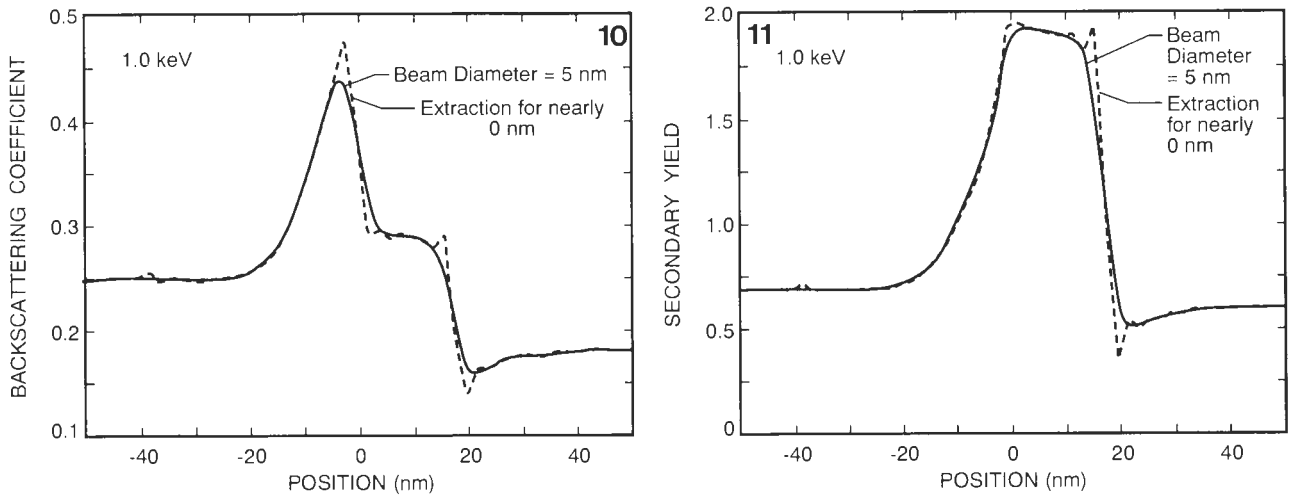

Figures 10 and 11. Simulated backscattering coefficient (**Fig. 10**) and secondary yield (**Fig. 11**) as a function of position for a 1 μm step in a silicon substrate. The beam energy is 1 keV. The solid line is for 5 nm beam diameter, while the dashed line is extracted from it as an approximation for zero beam diameter. The zero of position is the top of the ledge, and the wall angle is 89°.

---

signal $s(x_0,d)$ obtained with the Gaussian-distributed beam centered at x_0 and with diameter d is given by [21]:

$$s(x_0,d) = \frac{2.56}{\sqrt{2\pi}\, d} \int_{x_0-a}^{x_0+a} \exp[-3.28(x-x_0)^2/d^2]\, s_0(x)dx, \tag{1}$$

where $s_0(x)$ is the signal obtained from an electron beam with zero beam diameter at position x and a = 1.56 d. The beam diameter is determined by convention [20] as the diameter of the circle containing 56% of the current, and the extent of the integral is four standard deviations about x_0. Note that the area under a one-dimensional Gaussian distribution of the form of eq. (1) is 80% between -d/2 and d/2. The definition of beam diameter relies on this fact because it is usually determined experimentally by moving the beam across an edge and measuring the signal, which has a one-dimensional Gaussian distribution. To implement eq. (1), a profile is first simulated with a beam diameter of zero and a small enough point spacing that the target features are sufficiently well represented. The profile is then interpolated linearly between the calculated points to obtain at least 100 points in the integral, which is then solved with an available integration routine.

The results for the case of the silicon ledge discussed at the beginning of this section are shown in Figures 8 and 9. The backscattering detector is now assumed to collect all the electrons. The backscattering coefficient, shown in Figure 8, is seen to broaden, as expected, with increasing beam radius from zero to 15 nm in increments of 5 nm. Notice that the noise is removed by the integration, which shows that it is much more efficient to obtain simulated profiles for finite beam diameters from one careful simulation at zero beam diameter. Note also that the appearance of the profile as the beam traverses the face of the ledge is greatly affected by the beam diameter, changing from a flat plateau to a sloping decline. Figure 9 shows the secondary yield for the same case as in Figure 8. The effect of increasing beam diameter is similar, but less pronounced for the secondaries because the edge profile has less structure.

Equation 1 can also be the basis for extracting a signal that more closely approximates one obtained with a beam with zero diameter from one measured with a finite beam diameter. If the pixel separation is small compared with the beam diameter, and if electronic noise and spatial jitter are sufficiently small, one can invert eq. (1) and construct a sharper signal. The beam-spread signal centered at x_i, $s(x_i, d)$, can be approximated by the sum of signals $s_0(x_j)$ with zero beam diameter at and on either side of the pixel located at x_i. This is a pixel discretization of eq. (1), which turns the integral into a finite sum of terms:

$$s(x_i,d) = C \sum_{j=i-n}^{i+n} \exp\,(-3.28\,(x_j-x_i)^2/d^2)\; s_0(x_j), \tag{2}$$

where C is the normalization constant given by:

$$C = [1 + 2\sum_{j=2}^{n+1} \exp(-3.28\ (x_j - x_1)^2\ /d^2)\ ]^{-1}, \quad (3)$$

and the value of the pixel separation must be constant. The value of n is determined by the noise level in $s(x_i,d)$. The extent of the sum must be restricted so that all the terms in the sum remain above the noise level. Otherwise the matrix inversion can become unstable (see textbooks on matrix solutions for a discussion of ill-conditioned matrices). Commonly, the signal-to-noise ratio is about 10, and one would set n such that:

$$x_n \leq x_1 + d[-\ln(0.1)/3.28]^{0.5}. \quad (4)$$

For a less noisy signal, n could be increased. The points x_i extend over the range of m data points, and an (m - 2n) by (m - 2n) banded matrix of bandwidth 2n + 1 results from the series of equations obtained from eq. (2) for all x_i. The matrix is then solved for all $s_0(x_i)$, i = 1, m - 2n in terms of the values of $s(x_i,d)$. There is a problem for rows in which the column extent would exceed the limit of 1 to m - 2n. For example, the first row would contain entries for $s_0(x_j)$, $j < 1$. For this row, the unknown values for $s_0(x_j)$ must be replaced with $s(x_j,d)$. The same procedure is applied to all rows having this problem. This introduces some error, especially near the end points of the trace, which is minimized if the signal is nearly constant near the ends.

The solutions for $s_0(x_i)$ have been obtained from the simulated data of Figures 8 and 9 for backscattering coefficient and secondary yield for a 1 μm step in a silicon substrate by using an available matrix solver. Plots of the results are shown in Figures 10 and 11. The solid lines correspond to the results for a 5 nm beam diameter from Figure 8 or 9. The dashed lines are the results from eq (2) with a 2 nm pixel separation. The dashed lines are in much closer agreement with the solid lines in Figures 8 and 9 for zero beam diameter, which demonstrates the utility of the method to reconstruct the finer detail associated with signals from a beam with smaller beam diameter.

Efficient use of Monte Carlo codes

The primary reluctance by SEM users to adopt Monte Carlo models as part of routine signal analysis is the relatively long running times of the codes even on present-day work-stations. However, these times can be greatly reduced if only the most important features of the signals are modeled. There is no need to reproduce the relatively slowly varying signals on either side of an edge to determine the edge position from the simulation. One can also benefit from past simulations so that a collection can be compiled for future reference. It is also good practice to use coarse point separation to assess the features of a target before using fine point separation for the regions of most interest. It was shown in **Effect of Beam Spreading** above, that it is much more efficient to use a simulated signal obtained with zero beam diameter as the basis for simulations for any finite beam diameter. It is also possible to reconstruct simulations for any detector parameters by using a file containing the trajectories and energies of the outgoing electrons. Thus, one can minimize the actual running times of Monte Carlo codes by avoiding unnecessary recalculation of the signals or calculation of unnecessary target regions.

Another problem with using Monte Carlo code is that it is difficult to model the electric and magnetic fields that occur between the target and detectors. These fields can result from electronic lenses or from charging of the target. In principle, these effects can be modeled and accounted for, but in practice it is much more difficult because these effects depend on operating conditions, which change from sample to sample and from machine to machine. Therefore, discrepancies can occur between measurement and prediction due to these effects, which can cause the user to question the validity of the Monte Carlo code itself. Although these effects cannot be totally eliminated, some progress has been made [5, 9], and this area remains a fertile one for future research. Success, however, depends on the SEM manufacturers' cooperation and collaboration with those performing the modeling because instrument design plays an important role in determining the nature and magnitude of these effects.

Conclusions

In conclusion, Monte Carlo computer codes have been written that can simulate the signals produced by a line-edge in the SEM in either two or three dimensions. Use of these simulations in conjunction with high-accuracy SEM measurements was shown to give edge positions to an uncertainty of less than 10 nm. Simulations were performed for photoresist lines on a silicon substrate coated with a layer of photoresist for antireflection. A simulation has been obtained for incident electrons with zero beam diameter. This simulation has then been used to construct simulations for finite beam diameters. A method was also derived for extracting data corresponding to zero beam diameter from data measured with a finite beam diameter.

Approaches were formulated for the efficient use of Monte Carlo codes and possible sources of discrepancies between measurements and predictions were examined. The computer software discussed in this paper is avail-

able to anyone; inquiries should be sent to the author, who will assist the user in implementing these codes.

Acknowledgments

This work was supported in part by the NIST National Semiconductor Metrology Program. The authors wish to thank G. William Banke of IBM, Essex Junction, VT, for his fabrication of the silicon-step specimen and Neal Sullivan of Digital Electronics Corp., Hudson, MA, for his suggestion to study the photoresist lines. He also thanks Michael Postek and Andras Vladar (now at Hewlett Packard, Palo Alto, CA) of NIST for their work in performing the high-accuracy measurements used in this paper.

References

[1] Archard GD (1961) Backscattering of electrons. J Appl Phys **32**: 1505-1510.

[2] Bakaleinikov LA, Tretyakov VV (1995) The influence of elastic and ionization cross-section approximations on the result of Monte Carlo calculations. Scanning **17**: 243-249.

[3] Browning R, Li TZ, Chui B, Ye Jun, Pease RFW, Czyzewski Z, Joy DC (1994) Empirical forms for the electron/atom elastic scattering cross sections from 0.1 to 30 keV. J Appl Phys **76**: 2016-2022.

[4] Browning R, Li TZ, Chui B, Ye Jun, Pease RFW, Czyzewski Z, Joy DC (1995) Low-energy electron/atom elastic scattering cross sections from 0.1-30 keV. Scanning **17**: 250-253.

[5] Davidson M (1994) Metrology models and simulation. In: SPIE'S Handbook of Critical Dimension Metrology and Process Control. Monahan K (ed.). SPIE Optical Engineering Press, Bellingham, WA. pp. 268-315.

[6] Gauvin R, Hovington P, Drouin D (1995) Quantification of spherical inclusions in the scanning electron microscope using Monte Carlo simulations. Scanning **17**: 202-219.

[7] Joy DC (1988) An introduction to Monte Carlo simulations. In: EUREM 88. Inst Phys (Bristol, UK) Conf Ser. **93**: 23-32.

[8] Joy DC (1995) A database on electron-solid interactions. Scanning **17**: 270-275.

[9] Joy DC, Joy CS (1995) Dynamic charging in the low voltage SEM. J Microsc Soc Am **1**: 109-112.

[10] Joy DC, Luo S (1989) An empirical stopping power relationship for low-energy electrons. Scanning **11**: 176-180.

[11] Kotera M, Ijichi R, Fujiwara T, Suga H, Wittry D (1990) A simulation of electron scattering in metals. Jap J Appl Phys **29**: 2277-2282.

[12] Lowney JR (1995) MONSEL-II: Monte Carlo simulation of SEM signals for linewidth metrology. Microbeam Analysis **4**: 131-136.

[13] Lowney JR (1995) Use of Monte Carlo modeling for interpreting scanning electron microscope. Linewidth Measurements. Scanning **17**: 281-286.

[14] Lowney JR (1996) Monte Carlo simulation of scanning electron microscope signals for lithographic metrology. Scanning **18**: 301-306.

[15] Lowney JR, Banke GW, Gauvin R, Howitt D, Joy DC, Nunn J, Radimski Z, Sartore R (1995) Workshop Report 2: Monte-Carlo models for predicting edge positions from scanning electron microscope signals. In: Microbeam Analysis (1995). VCH Publishers, New York. pp. 341-342.

[16] Lowney JR, Postek MT, Vladar AE (1995) Workshop Report 3: Edge positions from scanning electron microscope signals by comparing models with measurements. In: Microbeam Analysis (1995). VCH Publishers, New York. pp. 343-344.

[17] Lowney JR, Vladar AE, Postek MT (1996) High-accuracy critical-dimension metrology using a scanning electron microscope. In: Metrology, Inspection, and Process Control for Microlithography X. Proc. SPIE **2725**: 515-526.

[18] Ly TD, Howitt DG, Farrens MK, Harker AB (1995) Monte Carlo calculations for specimens with microstructures. Scanning **17**: 220-227.

[19] Murata K, Yasuda M, Kawata H (1995) Effects of the introduction of the discrete energy loss process into Monte Carlo simulation of electron scattering. Scanning **17**: 228-234.

[20] Myklebust RL, Newbury DE (1995) Monte Carlo modeling of secondary X-Ray fluorescence across phase boundaries in electron probe microanalysis. Scanning **17**: 235-242.

[21] Myklebust RL, Newbury DE, Yakowitz H, (1976) NBS Monte Carlo electron trajectory calculation program. In: Proc. Workshop on Use of Monte Carlo Calculations in Electron Probe Microanalysis and Scanning Electron Microscopy. Heinrich K, Newbury D, Yakowitz H (eds.). NBS Spec. Publ. 460. Available from National Technical Information Service (NTIS), Springfield, VA. pp. 105-125.

[22] Newbury DE, Joy DC, Echlin P, Fiori CE, Goldstein JI (1986) Advanced Scanning Electron Microscopy and X-Ray Microanalysis. Plenum Press, New York. pp. 19-43.

[23] Nunn JW (1995) Application of Monte Carlo modeling in the measurement of photomask linewidths at the national physical laboratory. Scanning **17**: 296-301.

[24] Postek MT, Vladar AE, Banke GW, Reilly TW (1995) Workshop Report 1: Scanning electron micro-

scope metrology as related to a defined edge structure. In: Microbeam Analysis 1995. VCH Publishers, New York. pp. 339-430.

[25] Radzimski ZJ, Russ JC (1995) Image simulation using Monte Carlo methods: Electron beam and detector characteristics. Scanning **17**: 276-280.

[26] Reimer L (1985) Scanning Electron Microscopy. Springer-Verlag, New York. pp. 75-116.

[27] Semiconductor Industry Association (1994) The National Technology Roadmap for Semiconductors. Semiconductor Industry Association, 4300 Stevens Creek Boulevard, Suite 271, San Jose, CA 95129. pp. 83-85.

[28] Vladar AE, Postek MT, Davilla SD (1995) Is your scanning electron microscope hi-fi? Scanning **17**: 287-295.

Discussion with Reviewers

R.G. Sartore: You mention that edge slope, surface roughness and rounding can cause smearing of the measured signal. Is there any estimate or measurements possible of the expected uncertainty due to these factors that you mention?
Author: The Monte Carlo code can simulate the effects of edge slope and to some degree estimate the effects of roughness and rounding. However, it is very time consuming to perform the calculations and measurements needed to identify and quantify these effects. Therefore high-quality samples are needed to obtain the best metrology.

R.G. Sartore: In the fitting of measured data to the simulated signals, you quantify the uncertainty in the horizontal direction for the curve fit. Could you elaborate on some of the other components that could be expected to significantly impact the accuracy of the measurement?
Author: The uncertainty is determined by overlaying the experimental and simulated signals. Thus, the shape of the signals must be properly measured and simulated both in amplitude and position. This requires a very well controlled and calibrated instrument as well as correct model and theory for the simulation. Such parameters as detector and amplifier linearity as well as collected electrons that are not accounted for in the model can cause increased uncertainty in the analysis.

R.G. Sartore: In the solution of the inverse problem for beam size, you have demonstrated how to successfully reconstruct the finer details of zero beam width signal from a finite beam width signal. Have you applied this same technique to measured data? If so, what is the additional difficulty in implementing this procedure to measured data and how dependent is it on the physical measurement of beam diameter?
Author: The application to measured data, which I have performed since writing this paper, is straightforward, but has not yielded much new information from the data because of the presence of noise in the data. Noise reduces the stability of the matrix inversion and forces there to be fewer terms in the sum given in eq. (3), thus, worsening the approximation and the results form the inversion. I am presently working on methods to reduce the effects of noise in the data. It is also important to have a good estimate of the beam diameter.

R.G. Sartore: You mention the importance of obtaining good information from instrumentation manufacturers to successfully model electron/instrument interaction. What type of information would you like to see from the manufacturers? Is it feasible to list this data in instrument specifications so that potential buyers could run simulations of performance under expected use conditions?
Author: It is very important that the user of a SEM knows how his instrument works from the electron gun to the display image if he is going to be able to model the image correctly. Many researchers are trying now to develop models that can take into account the different instrument systems that are being used in modern SEMs such as different detectors and lens designs.

K. Murata: You scaled and shifted the experimental data to obtain the best agreement by eye. I think it is important to know the exact zero of position of the sample for future study. Could you comment on how accurately you can achieve position measurements?
Author: The simulation is based on a known model input for the target with a given zero of position. The sample was very close in form to the model target except for the presence of some roughness, rounding, and possible contamination. It is difficult to state quantitatively how large these effects are, but they were seen to be small in cross sectional measurements relative to the stated uncertainty in position.

K. Murata: What type of detector is used in your experiments?
Author: A microchannel plate was used to detect the backscattered electrons (BSEs), and both the microchannel plate and an Everhart-Thornley (ET) detector were used to detect secondary electrons (SEs). The contribution of BSEs to the SE signal from the microchannel plate was very small as learned from comparison with the signals from the ET detector and from the overall agreement in shape with the simulations since the signals were very different between BSEs and SEs across the edge.

K. Murata: You have obtained very good agreement between experiment and simulation for the secondary electron signals. Do the secondaries produced at the chamber wall by the backscattered electrons not significantly influence the secondary electron signal?
Author: The secondaries produced by the backscattered electrons that collide with chamber walls and pole piece can affect the secondary signal. The shadowing of the chamber by the microchannel plate reduces this effect, and the agreement between the microchannel plate and ET detectors implies that the contribution of this effect is probably small. The overall agreement between measurement and simulation also implies that the effect is small.

K. Murata: You investigated the signal mainly at low primary beam energies. Could you comment on what advantage they have, compared to high energies?
Author: Low primary beam energies are preferred because they cause less damage to the sample, less charging, and penetrate less distance into the target. In principle, low-energy signals show greater target detail and can lead to greater accuracy. However, they can have larger beam diameters and be more susceptible to contamination and other surface effects.

K. Murata: Please explain how you handled the reflection of the secondary electrons re-entered on the sample surface. For example, from where did you quote the reflection coefficient?
Author: The secondaries were treated in the same way as the backscattered electrons. Those that re-enter the sample scatter from target atoms and can re-emerge. Quantum mechanical effects associated with the wave nature of the secondary electrons were not included in this calculation.

D.C. Joy: A practical problem in low energy metrology is that the probe is not Gaussian because of chromatic aberration tails. Can these effects be taken into account in this code?
R. Gauvin: Will your deconvolution work well for a non-Gaussian beam: for example, for a distribution which has significant tails because of aberration effects in the final probe size? Does this effect become important for beam energies below 1 keV?
Author: If a better model for the beam distribution is determined, it can be included in the Monte Carlo code through a modification in the routine that determines the positions of the incident electrons. The deconvolution formulism can also be easily modified to account for non-Gaussian beam profiles, which can occur at low energies. However, the stability of the matrix inversion may be affected, which could reduce the ability to resolve fine structure.

D.C. Joy: You note that in MONSEL-III you can model finite three-dimensional structures as a collection of linear features. Might it be possible instead to use a computer-aided design (CAD) representation of the structure to permit a more general and flexible description?
Author: MONSEL-III is based on a fixed target geometry, and the equations used to determine boundary crossings by the electrons are limited to this geometry. In principle, it is possible to mate the routines to CAD representations of the targets, but this would require more work.

D.C. Joy: You demonstrate that a precision of just a few parameters is achievable using the Monte Carlo method. Since Monte Carlo simulation is a continuum model of the specimen, how much smaller detail can we expect the Monte Carlo method to model before it becomes unphysical?
Author: The physical assumptions in these Monte Carlo codes imply that the target is large when compared with atomic separations and that the electrons are not affected by quantization associated with target boundaries. Thus, it is not possible to use these codes for features much smaller than those discussed in this paper. New approaches will have to be developed to describe features below about 5 nm.

Z.J. Radzimski: It is practically impossible to simulate the intensity of SE emission for "real" SEM samples due to contamination build-up and other surface contamination effects. On the other hand, critical-dimension (CD) measurement techniques rely primarily on the shape of a profile and not on intensity. How much can the SE simulation methods be simplified and still be useful from this application point of view?
Author: The intensities of the measured and simulated emissions need not be the same, and in this work, the data were scaled to agree with the simulations because the measurements were not absolute. However, it is necessary to have a good model for either the energy loss or exit depth of secondaries because the shape of the SE signals can depend on them.

Z.J. Radzimski: Which mode of imaging, BSE or SE, will give better resolution for measurements of 0.1 μm lines? Can Monte Carlo methods give reasonable answers to this question? How far can they be useful to predict the optimum value of electron beam energy and diameter?
Author: The width of the bright "blooming" feature on SE signals is broader than that on BSE signals, and this

could lead to reduced resolution as has been shown experimentally. However, from the standpoint of the Monte Carlo modeling, the fits for SE and BSE can, in principle, yield comparable resolution. Measurement issues also could cause one to be preferred over the other. The physical models are more accurate for BSE, and this is one reason to prefer BSE. Generally, one would want to use low beam energies and small diameters although these two needs can conflict. The codes can be used to determine an optimum trade-off between them.

R. Gauvin: What will be the effect of computing the beam diameter with 90% of the electrons on your deconvolution technique since this is the convention for several researchers?
Author: Increasing the beam diameter to include 90% of the electrons will not change anything in principle except for the numbers in eqs. (1-3), but in practice, it could make the matrix inversion less stable because of the increase in the width of the band of the matrix.

R. Gauvin: What do you think about Monte Carlo simulations which model electrons as particles when the electron energy is below 1 keV, which is the case in your code as well as in my codes? Do you think we should model electrons by using a wave description instead?
Author: Treating the electrons as waves and solving a quantum-mechanical scattering problem that performs a complete partial wave analysis with appropriate boundary conditions is extremely formidable even in the case of semiconductor transport where the energies are low enough that the effective masses are well known. For the case of secondary electrons, a calculation based on the full band structure would be needed, which would be beyond today's calculational capabilities. For backscattered electrons, the energies are above 50 eV, and quantum effects are usually small, but they do occur for the secondaries. My codes use extrapolations down from the higher-energy formalisms, and the predictions still agree well with measurements, but there should be more studies regarding the onset of quantum effects.

R. Gauvin: Do you think that channeling may affect the secondary and backscattering electron profiles?
Author: Channeling can certainly affect the profiles, and it is difficult to model the effects because of the need to include the lattice configuration in the scattering problem. In a thick target, channeling should be a small problem, but in a thin film, it could be very important if the beam is aligned with a lattice plane.

R. Gauvin: I think that carbon contamination will reduce the precision of your deconvolution technique. Can you comment about ways of minimizing or eliminating contamination in the SEM?
Author: Contamination is a real problem in SEM measurements, and very high vacuum would reduce it. Beam currents and voltages also should be kept as low as possible. Specimens themselves can be contaminated, of course, and it is difficult to clean them.

R. Gauvin: Since the electron detector response functions must be known if we want to apply your method in practice, can you give some ideas about the way we can experimentally measure their efficiency?
Author: I think you could place the detector in the place of the target and measure the signal as the beam is scanned in energy while the current is held fixed.